Magnetic circular dichroism and absorption spectra of *f–f* transitions $^5I_8 \rightarrow {}^5F_2$ and $^5F_3$ in the $HoFe_3(BO_3)_4$ single crystal

Cite as: Low Temp. Phys. **46**, 734 (2020); https://doi.org/10.1063/10.0001371
Submitted: 20 May 2020 . Published Online: 30 July 2020

A. V. Malakhovskii, V. V. Sokolov, and I. A. Gudim

Low Temperature Physics ARTICLE scitation.org/journal/ltp

Magnetic circular dichroism and absorption spectra of f–f transitions $^5I_8 \rightarrow {}^5F_2$ and $^5F_3$ in the $HoFe_3(BO_3)_4$ single crystal

Cite as: Fiz. Nizk. Temp. **46**, 869–876 (July 2020); doi: 10.1063/10.0001371
Submitted: 20 May 2020

A. V. Malakhovskii,[a] V. V. Sokolov, and I. A. Gudim

AFFILIATIONS

Kirensky Institute of Physics, Federal Research Center Krasnoyarsk Scientific Center, Siberian Branch, Russian Academy of Sciences, Krasnoyarsk 660036, Russia

[a]**Author to whom correspondence should be addressed:** malakha@iph.krasn.ru

ABSTRACT

Magnetic circular dichroism (MCD) and absorption spectra of multiferroic $HoFe_3(BO_3)_4$ of $^5I_8 \rightarrow {}^5F_2$ and $^5F_3$ f–f transitions are measured at $T = 90$ K. The absorption spectra are expanded into Lorentzian components, and the transition intensities are obtained. The Zeeman splitting of some transitions is determined using the MCD and absorption spectra. The MCD spectra and Zeeman splitting are theoretically analyzed in the free-atom $|J, \pm M_J\rangle$ wave function approximation by using the concept of a crystalline quantum number. An inconsistency is revealed when this concept is applied to ions with an integer moment, and a modification of the concept is proposed. Anomalously intense vibronic repetitions of electronic transitions from excited sublevels of the ground multiplet are found.

1. INTRODUCTION

Like most ferroborates, the $HoFe_3(BO_3)_4$ crystal belongs to the class of multiferroics.[1,2] It has a huntite structure with the trigonal symmetry $P3_121$ (D_3^4), which transforms into the $R32$ symmetry at temperatures above 360 K, for single crystals grown from a solution in a melt.[3] The local symmetry of the holmium ion is D_3 in the $R32$ space group and C_2 in the $P3_121$ space group. The $HoFe_3(BO_3)_4$ crystal becomes an easy-plane antiferromagnet at $T = 38$ K. A spin-reorientation transition to the easy-axis phase takes place as the temperature decreases to 4.7 K.[4,5]

The $HoFe_3(BO_3)_4$ absorption spectra in the 500–1000 cm^{-1} infrared range were studied in Ref. 3. The f–f transition spectra in the 8500–24500 cm^{-1} range over a broad temperature interval, which includes the reorientation transition, were studied in Ref. 6, and were also investigated as functions of the magnetic field in Ref. 7.

Magnetic circular dichroism (MCD) consists of paramagnetic and diamagnetic components. The temperature dependence of the paramagnetic MCD f–f transitions deviates from the Curie–Weiss law,[8–10] due to the nature of the f–f transition's permission. Diamagnetic MCD is caused by Zeeman splitting of transitions and makes it possible to experimentally determine these cleavages even when they are not directly observed.[11–13] This article concerns the study of the diamagnetic effect in $HoFe_3(BO_3)_4$. The interpretation of this effect in the holmium ion with integer momentum has revealed several features that stand out in comparison to ions with a half-integer momentum.

2. EXPERIMENTAL TECHNIQUE

The $HoFe_3(BO_3)_4$ single crystal was grown from a bismuth trimolybdate solution-melt with a non-stoichiometric composition of crystal-forming oxides, the technology for which is described in detail in Ref. 6. The lattice constants of $HoFe_3(BO_3)_4$ are: $a = 9.53067$ (5) Å, $c = 7.55527$ (6) Å.[5] The unit cell contains three formula units. Holmium ions occupy only one type of position: they are located in the center of trigonal prisms with C_2 symmetry that consist of six oxygen ions. The FeO_6 octahedra are connected by common edges so helicoidal chains extend parallel to the C_3 axis that are independent of each other.

The absorption spectra were measured by the two-beam technique using an automated spectrophotometer designed based on the DFS-8 diffraction monochromator. The optical width of the gap (spectral resolution) was 0.2 Å. The absorption spectra were measured as the light propagated perpendicular to the crystal's C_3 axis, for the light-wave electric vector **E** parallel (π-spectrum) and perpendicular (σ-spectrum) to the C_3 axis, and as the light propagated along the C_3 axis (α-spectrum). The absorption spectra measured in

σ- and α-polarizations coincide with each other within the experimental error. This means that the absorption occurs primarily through the electric dipole mechanism.

The magnetic circular dichroism (MCD) spectra were recorded as light propagated along the C_3 axis of the crystal. A magnetic field of 5 kOe was also directed along the C_3 axis. The circular dichroism was measured with light-polarization modulation using a piezoelectric-modulator.[10] The MCD was measured as the half difference of the circular dichroisms for plus and minus magnetic fields. Therefore, natural circular dichroism was excluded in this case. The sensitivity when measuring the circular dichroism was 10^{-4}, and the spectral resolution was the same as that for the absorption spectra. The sample was placed in a nitrogen-gas-flow cryostat. The temperature measurement accuracy was about 1 K. The thickness of the $HoFe_3(BO_3)_4$ samples was 0.19 mm.

3. RESULTS

The polarized absorption spectra and MCD of $^5I_8 \rightarrow {}^5F_3$ and $^5F_2$ absorption bands at 90 K are shown in Fig. 1 and Fig. 2. The absorption spectra are decomposed into Lorentzian components, and their intensities are determined (see Table I). The uppercase letters in Figs. 1 and 2 designate transitions from the ground state, and lowercase letters indicate transitions from the upper sublevels of the ground multiplet or vibronic transitions. In the $HoFe_3(BO_3)_4$ crystal, holmium ions are located in positions with C_2 symmetry. However, the number of absorption spectra splitting components and their polarization are well described by D_3 symmetry in the first-approximation, and sometimes even by cubic symmetry.[6] Therefore, transitions from both the ground and excited sublevels of the ground multiplet were identified based on the transitions' polarization, according to D_3 symmetry selection rules (Table II).

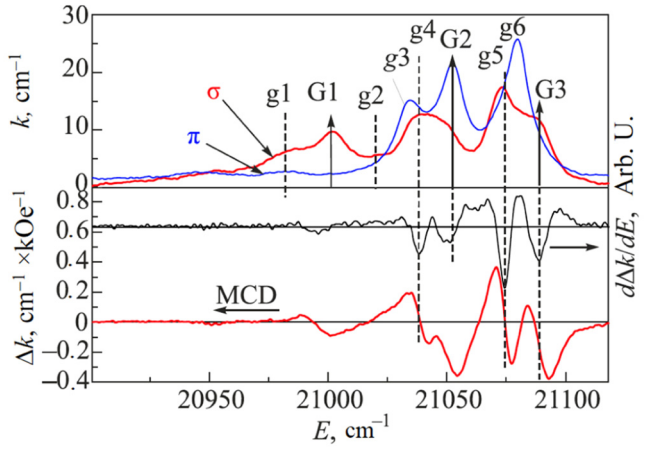

FIG. 1 Polarized absorption spectra (k), the magnetic circular dichroism (Δk), and the dichroism derivative ($d\Delta k/dE$) of the $^5I_8 \rightarrow {}^5F_2$ (G) transition at a temperature of 90 K.

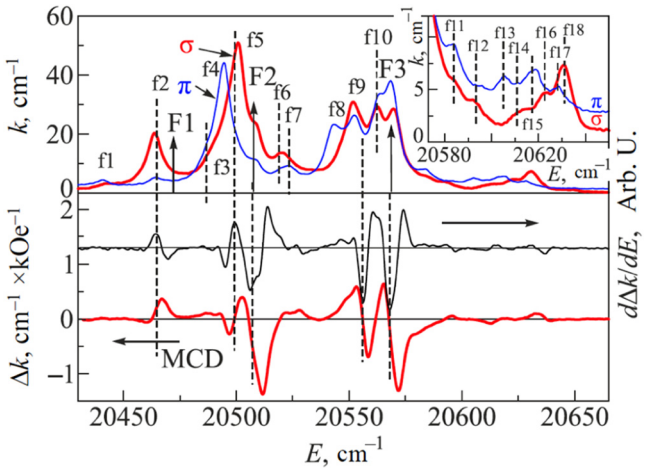

FIG. 2 Polarized absorption (k), magnetic circular dichroism (Δk), and dichroism derivative ($d\Delta k/dE$) spectra of the $^5I_8 \rightarrow {}^5F_3$ (F) transition at a temperature of 90 K.

The MCD of the doublet in a magnetic field directed along the propagation of light is determined by the following expression:

$$\Delta k = k_{m+}\phi(\omega, \omega_0 + \Delta\omega_0) - k_{m-}\phi(\omega, \omega_0 - \Delta\omega_0). \quad (1)$$

Here, k_{m+} and k_{m-} are the amplitudes of the (+) and (−) circularly polarized absorption lines; φ are polarized line shape (+) and (−) functions. If the Zeeman splitting $\Delta\omega_0$ is much smaller than the line width, then

$$\Delta k = k_m c\phi(\omega, \omega_0) + k_m \Delta\omega_0 \partial\phi(\omega, \omega_0)/\partial\omega_0. \quad (2)$$

Here, $k_m = k_{m+} + k_{m-}$ is the amplitude of the line not split by the magnetic field and $c = (k_{m+} - k_{m-})/k_m$. The first term in Eq. (2) is the paramagnetic MCD, and the second is the diamagnetic MCD. The fine structure of the MCD spectra (Figs. 1 and 2) is driven by the diamagnetic effect. The integral of the MCD spectrum over the multiplet gives the integral paramagnetic MCD of the multiplet (the integral with respect to the diamagnetic part is obviously equal to zero).

The diamagnetic MCD of the individual lines is not always spectrally resolved. However, it is possible to determine the signs of the diamagnetic MCD ($\Delta\omega_0$) by using the first derivative of the MCD. For the MCD written in the form of Eq. (1), it can be shown[8] that the signs of the maxima along function $\partial\Delta k/\partial\omega$ at the positions of the absorption lines provide the signs of the diamagnetic effect ($\Delta\omega_0$). Thus, we find the signs of the diamagnetic transition effects from the experimental MCD spectra (Figs. 1, 2 and Table I). Obviously, purely π-polarized lines do not have MCD.

If the transition spectra are well resolved, the Zeeman splitting $\Delta\omega_0$ can be found by using the absorption and MCD spectra. According to Ref. 8, for a Lorentzian absorption line (as is the

TABLE I. The energies of the levels and transitions (E), intensities of transitions in π- and σ- polarizations (I_π, I_σ), and the experimentally measured changes of the Landé factor along the C_3 axis during the transition (Δg_C). The symbols π and σ in the columns (I_π, I_σ) mean that the lines with this polarization are very weak and their intensity is not defined.

Multiplets	Levels, transitions	E, cm^{-1}	$I\pi$, cm^{-2}	$I\sigma$, cm^{-2}	Δg_C
$^5I_8$ (Gr)	Gr1 ($E1$)	0			
	Gr2 (A)	8–9			
	Gr3 (A)	14			
	Gr4 (A)	16–17			
	Gr5 (E)	20–21			
	Gr6 (A)	46–48			
	Gr7 (A)	52–58			
	Gr8 (A)	68–70			
$^5F_3$ (F)	F1 ($A2$)	20472	0	σ	?
	F2 ($E2 + A$)	20509	56	50	–45
	F3 ($E1 + A$)	20570	308	254	–12.3
	f1 (Gr8 → F2)	20441	32	46	?
	f2 (Gr6 → F2)	20464	36.3	239	+ 4.5
	f3 (Gr5 → F2)	20488	120	126	?
	f4 (Gr8 → F1 + 90)	20494	426	0	0
	f5 (Gr2 → F2)	20500	0	739	+ 1.8
	f6 (Gr6 → F3)	20521	26	154	?
	f7 (Gr8 → F1 + 120)	20524	38	0	0
	f8 (Gr3 → F1 + 85)	20543	197	0	0
	f9 (Gr5 → F3)	20550	203	430	?
	f10 (Gr2 → F3)	20562	249	213	?
	f11 (Gr3 → F2 + 84)	20584	45	46	?
	f12 (F2 + 84)	20593	9	17	(–)
	f13 (Gr6 → F3 + 82)	20605	25.3	0	(–)
	f14 (Gr5 → F2 + 122)	20610	π	24	(+)
	f15 (Gr4 → F2 + 124)	20617	20	0	?
	f16 (Gr8 → F3 + 120)	20622	0	37	(+)
	f17 (F2 + 119)	20628	17	35	?
	f18 (Gr5 → F3 + 82)	20631	0	39	(–)
$^5F_2$ (G)	G1 ($A1$)	21002	0	178	
	G2 ($E2$)	21052	346	55	(–)
	G3 ($E1$)	21090	19	102	–10.1
	g1 (Gr8 → G2)	20983	0	167	
	g2 (Gr8 → G3)	21020	0	30	
	g3 (Gr6 → G1 + 79)	21034	241	0	0
	g4 (Gr4 → G2)	21038	0	207	(–)
	g5 (Gr4 → G3)	21073	0	266	–4.1
	g6 (Gr6 → G1 + 125)	21080	325	0	0

Note: The symmetries of states or the identification of transitions from the upper states of the ground multiplet are shown in parentheses in Table I.

TABLE II. D_3 symmetry selection rules for electric dipole transitions. .

	A_1	A_2	E
A_1	–	π	σ(α)
A_2	π	–	σ(α)
E	σ(α)	σ(α)	π, σ(α)

case here), this looks like

$$\Delta\omega_0 = 2\frac{\Delta k_{dm}}{k_m}|\omega_m - \omega_0|. \quad (3)$$

Here, Δk_{dm} and ω_m are the magnitude and position of the MCD diamagnetic line extrema, respectively, and k_m is the absorption amplitude of the α-line. The experimental changes in the Landé factor Δg_C at the transitions (Table I) were found from the Zeeman splitting of transitions in a magnetic field directed along the C_3 axis of crystals, by using expression

$$2\hbar\Delta\omega_0 = \mu_B H \Delta g_C. \quad (4)$$

4. DISCUSSION

The ground state of the holmium ion, $^5I_8$, at the transition to cubic and then to trigonal symmetry, is transformed as follows:

$$\begin{aligned} {}^5I_8(J=8) &\rightarrow A_1 + 2E + 2T_1 + 2T_2 \\ &\rightarrow A_1 + 2E + 2(A_1 + E) + 2(A_2 + E). \end{aligned} \quad (5)$$

The selection rules (Table II) make it possible to analyze the linear polarization of transitions, but not the circular polarization in a magnetic field. This possibility is provided by the concept of a crystalline quantum number for electronic states in crystals that have axial symmetry, proposed in Ref. 14. In trigonal crystal the crystalline quantum number μ for states with integer momentum assumes the following values: μ = 0, +1, −1. In addition, in uniaxial crystals the first-approximation can describe electronic states by the free-atom wave function $|J, \pm M_J\rangle$. The following correspondence exists between the values μ, M_J, and the irreducible representation of states:[14]

$$M_J = 0 \ \pm1 \ \pm2 \ (\pm3)_{1,2} \ \pm4 \ \pm5 \ (\pm6)_{1,2} \ \pm7 \ \pm8 \quad (6)$$

$$\mu = 0 \ \pm1 \ \mp1 \ 0 \ \pm1 \ \mp1 \ 0 \ \pm1 \ \mp1 \quad (7)$$

$$A_1 \ E_1 \ E_2 \ A_1,A_2 \ E_1 \ E_2 \ A_1,A_2 \ E_1 \ E_2 \quad (8)$$

The doublets E_1 and E_2 are distinguished by the μ sign. States such as $(\pm M_J)_{1,2}$ look like $|+M_J\rangle \pm |-M_J\rangle$. The projection M_J determines the state splitting in a magnetic field. Accordingly, the Landé factor g_{CM} of the doublet $\pm M_J$ in the $|J, \pm M_J\rangle$ wave function approximation is equal to:

$$g_{CM} = 2gM_J, \quad (9)$$

where g is the Landé factor of the free ion (Table III). Then, it is possible to theoretically evaluate the changes in the Landé factor Δg_{CM} due to the transition between states, which was done for rare-earth crystals with a half-integer momentum of ions.[8,12] For a number of transitions, there is a fairly good correspondence between theory and experiment, but there are also transitions for which the experiment and theory differ even in the sign of the effects.

TABLE III. Landé factors of states (g_{CM}) along the C_3 axis in the free-atom function $|J,\pm M_J\rangle$ approximation.

Symm.	$A_1(A_2)$	E_1	E_2	A_1,A_2	E_1	E_2	A_1,A_2	E_1	E_2
M_J	0	1	2	$(\pm3)_{1,2}$	4	5	$(\pm6)_{1,2}$	7	8
$^5I_8$ (Gr)	0	2.5	5	0	10	12.5	0	17.5	20
$^5F_3$ (F)	0	2.5	5	0					
$^5F_2$ (G)	0	2	4						

Ref. 14 provides the selection rules for the number μ in crystals, similar to the rules for M_J in free ions. In particular, for electric dipole transitions:

$$\begin{aligned}&\Delta\mu = \pm 1 \text{ corresponds to } \mp \text{ circular polarization}\\ &\text{and } \sigma - \text{polarized waves,}\\ &\Delta\mu = 0 \text{ corresponds to } \pi - \text{polarized waves.}\end{aligned} \tag{10}$$

For linearly polarized waves, these selection rules coincide with the rules in Table II. The selection rules (10) have made it possible to predict the magnitude and sign of a number of *f*–*f* transitions in Er^{3+} ions with a half-integer momentum.[12]

Another situation is observed for ions with integer momenta (see the diagram in Fig. 3). σ-polarized (and therefore, circularly polarized) *E*–*E* transitions are forbidden in accordance with the selection rules (10), which contradicts the experiment and the symmetry selection rules (Table II). Therefore, it is possible to conclude that the selection rules (10) for μ are not strict. Instead, selection rules (10) are strict only for M_J. For example, the transition $M_J = \pm 1 \rightarrow M_J = \pm 4$ is forbidden. However, states with different M_J but identical μ are mixed in the crystals. In particular, if the state $M_J = \pm 2$ is mixed with the state $M_J = \pm 4$, then the transition under consideration will be partially allowed. Thus, the splitting of states and transitions in a magnetic field is determined by the main part of the $|J, \pm M_J\rangle$ wave function, with $M_J = M_{\text{eff}}$, whereas the polarization and intensity of the transition are determined by the admixtures caused by the crystal field. The odd part of the crystal field mixes states with different parities, creating partial parity-allowance of *f*–*f* transitions. An even part of the crystal field mixes states with different M_J, thus ensuring allowance by M_J. As such, it is possible to explain cases when the experimental value of Zeeman splitting coincides with what is theoretically predicted, but the sign is opposite.

Based on the need to match the selection rules for electronic transitions between states, characterized by a crystalline quantum number μ and irreducible representations, rather than (10) we propose the following selection rules for μ, suitable for both states with integer and half-integer moments:

$$\begin{aligned}&\Delta\mu = \pm 1, \ \pm 2 \text{ corresponds to } \mp \text{ circular polarization}\\ &\text{and } \sigma - \text{polarized waves,}\\ &\Delta\mu = 0 \text{ corresponds to } \pi - \text{polarized}\\ &\text{waves or it is forbidden (Table II).}\end{aligned} \tag{11}$$

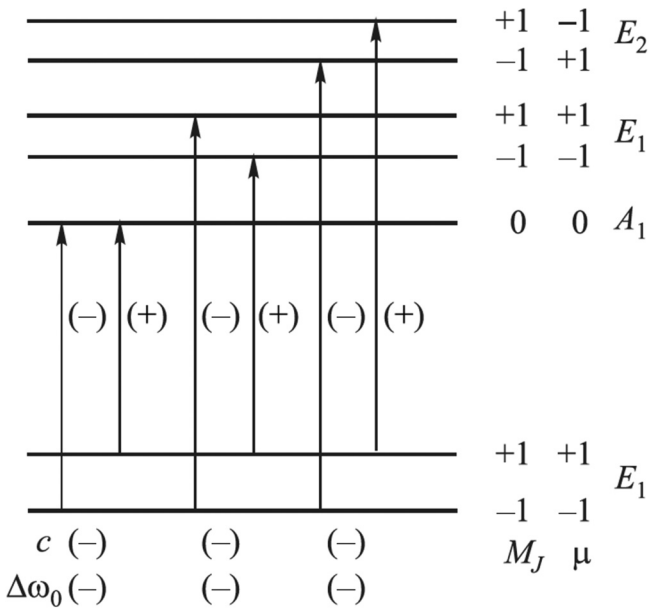

FIG. 3 Diagram of the main transition types and their polarizations, in ions with integer moments, taking into account the modified selection rules (11).

The diagram in Fig. 3 is created on the basis of selection rules (11). From the above consideration, it is clear that selection rules (10) and (11) are not strict, but allow room for a qualitative assessment of the situation. Figure 3 shows that the values of the Zeeman splitting of $E_1 \rightarrow E_1$ and $E_2 \rightarrow E_2$ transitions are equal to the sum of the splitting of the ground and excited states. The value of the Zeeman splitting of the $E_1 \leftrightarrow E_2$ transitions is the difference between the ground and excited state splitting, and its sign depends on the ratio of the Zeeman splitting of the ground to that of the excited state. In Table IV, diagrams that are similar to those shown in Fig. 3 are used to obtain the Zeeman splitting signs of all types of transitions. The first signs for the $E_1 \leftrightarrow E_2$ transitions relate to cases where the splitting of the ground state is larger than the splitting of the excited state.

TABLE IV. Signs of transitions Zeeman splitting. The first signs for the $E_1 \leftrightarrow E_2$ transitions relate to cases when the splitting of the ground state is larger than the splitting of the excited state. The absolute value of $E_1 \rightarrow E_1$ and $E_2 \rightarrow E_2$ transition splitting is equal to the sum of the splitting of the ground and excited states, whereas for the transitions $E_1 \leftrightarrow E_2$, this value is equal to their difference.

	A	E_1	E_2
$A\rightarrow$	0	(−)	(+)
$E_1\rightarrow$	(−)	(−)	(−,+)
$E_2\rightarrow$	(+)	(+,−)	(+)

4.1. The $^5I_8 \rightarrow {}^5F_2$ transition (G-band)

The polarized absorption and MCD spectra of the G-band are presented in Fig. 1. The excited $^5F_2$ state is split in the cubic and trigonal fields as follows:

$$\underset{}{^5F_2(J=2)} \rightarrow \underset{}{T_2 + E} \rightarrow \underset{\text{G1}}{A_1} + \underset{\text{G2}}{E} + \underset{\text{G3}}{E}. \tag{12}$$

The correspondence between the states in the trigonal field and states in the $|J, \pm M_J\rangle$ function approximation is easily seen from Eqs. (6)–(8), up to $M_J = 2$. The splitting of the G2 and G3 transitions due to a decrease in symmetry to C_2 is hardly detected even at 2 K.[15] The ground $^5I_8$ multiplet has $g = 1.25$. According to Ref. 4, the holmium ion in the $HoFe_3(BO_3)_4$ crystal has a magnetic moment $m = gM_J = 5\mu_B$ at $T = 2$ K. In this case, $M_J = 4$, and it follows from Eqs. (6)–(8) that the ground state has the symmetry E_1 and $g_{CM} = 2gM_J = 10$. According to Tables III and IV, transitions to the E-states of G2 and G3 (E_1 and E_2) should have negative Zeeman splitting, which is observed in the experiment (Table I).

It is worth paying special attention to the purely π-polarized lines g3 and g6. According to the selection rules (Table II), these are $A_1 \leftrightarrow A_2$ transitions, i.e., transitions from some kind of excited state. Going by symmetry, these could be transitions to the G1 (A_1) state, but their energy is less than the energy of G1. It remains to assume that the electron-vibrational transitions Gr6 (A_1) → G1 (A_1) + Vibr take place with participation of A_2 vibrations with energies of 79 and 125 cm^{-1} (Table I). The excited states of these transitions have the symmetry $A_1 \times A_2 = A_2$. Indeed, the theory in Ref. 16 has shown that the $HoFe_3(BO_3)_4$ crystal has these types of vibrations with similar energies. It must be emphasized that the purely electronic transition Gr6(A_1) → G1(A_1) is not observed, since it is forbidden not only in parity, but also in terms of selection rules (Table II). Usually, vibronic transitions in rare-earth ions are very weak, since the partially allowed *f–f* electronic transitions are repeated by even vibrations due to the weak difference in the adiabatic potentials of the ground and excited states. In the case under consideration, the odd component of the incompletely symmetric vibration A_2 allows the *f–f* transition, both in symmetry and parity. Vibrational parity-allowance of the *f–f* transition occurs, which is characteristic of 3*d* complexes.

The transition g5: Gr4 (A) → G3 (E) has a negative MCD (Table I). This means that the excited G3 doublet has E_1 type symmetry (Table IV). E_1 symmetry in state $^5F_2$ correspond to $g_{CM} = 2$ (Table III). Therefore, for the g5 transition, we have $\Delta g_{CM} = -2$. The experimental value is $\Delta g_{CM} = -4.1$ (Table I). If the G3 state has E_1 symmetry, then the G2 state has symmetry E_2 (6)–(8). According to Tables III and IV, the transition G3: Gr1 ($J = 8$, $M_J = 4$, $g_{CM} = 10$, E_1) → G3 ($J = 2$, $M_J = 1$, $g_{CM} = 2$, E_1) must have a negative Δg_{CM} equal in absolute value to the total g_{CM} of the initial and final states, i.e., $\Delta g_{CM} = -12$, which is close to the experimental value of −10.1 (Table I).

4.2. The $^5I_8 \rightarrow {}^5F_3$ transition (F-band)

The polarized absorption and MCD spectra of F-band are shown in Fig. 2. The excited $^5F_3$ state splits in the cubic and trigonal fields as follows:

$$^5F_2(J=3) \rightarrow A_2 + T_1 + T_2 \rightarrow \underset{\text{F1}}{A_2} + \underset{\text{F2}}{(A_1 + E)} + \underset{\text{F3}}{(A_2 + E)}. \tag{13}$$

The correspondence between the states in the trigonal field and states in the $|J, \pm M_J\rangle$ function approximation is easily seen from Eqs. (6)–(8), up to $J = 3$, and it should be noted that the representation A_2 corresponds to $\mu = 0$. The F1 line, assigned to the A_2 state transition, is very weak even at 2 K.[6] Its position is indicated by the arrow in Fig. 2. The splitting of the F2 and F3 transitions is very small, even at helium temperatures.[15] This means that the local symmetry in these excited states is almost cubic. At $T = 90$ K, states A and E in the F2 and F3 bands are indistinguishable. A number of weak vibronic lines (f11–f18) are observed, including two π-polarized lines f13 and f15 (Fig. 2, inset). Vibronic lines f12, f15, and f18 were observed earlier in Ref. 6 at low temperatures. The lines f11, f13, f14, f15, f16, and f18 are the vibronic repetitions of transitions from the excited states, made by local vibrations of 84 and 120 cm^{-1} (Table I, Fig. 2, inset). The purely π-polarized transitions f4, f7, and f8 (Table I) correspond to the $A_1 \leftrightarrow A_2$ transitions. As in the case of the G-band, this means that the initial state is one of the excited ground state singlets. The F2 and F3 multiplets contain singlets. However, if we consider the transitions to these multiplets, it is necessary to assume that the intensities of the $A \rightarrow E$ transitions that create the σ-polarization are zero, which is unlikely. The transitions to vibronic states F1 plus singlet vibrations are still left to consider. The possible identities of the transitions under consideration are presented in Table I. As in the case of the G-band, the purely electronic transitions that gave rise to vibronic transitions are not observed. This combination corresponds to centrosymmetric local symmetry and vibronic parity-allowance. It is worth noting that a weak *f–f* electronic transition with a strong vibronic satellite is observed only for transitions from the excited sublevels of the ground multiplet.

The transitions f2 (Gr6 – F2) and f5 (Gr2 – F2) occur from singlet states (Table I), F2 is the sum of states: F2 = $A + E$. The transition $A \rightarrow A$ is not split, but according to Tables IV and III, the transitions $A \rightarrow E_1$ and $A \rightarrow E_2$ for state $^3F_3$ should have $\Delta g_{CM} = -2.5$ and +5, respectively. A comparison of these results with the experiment shows that the state is F2 = $A + E_2$, and F3 = $A + E_1$.

Transition F3 consists of two transitions: Gr1 ($J = 8$, $M_J = 4$, $g_{CM} = 10$, E_1) → ($J = 3$, $M_J = 1$, $g_{CM} = 2.5$, E_1) with a theoretical value of $\Delta g_{CM} = -12.5$ (Tables III and IV), and the Gr1 transition ($J = 8$, $M_J = 4$, $g_{CM} = 10$, E_1) → A, with the theoretical value $\Delta g_{CM} = -10$. Both values are close to the experimental value −12.3. Therefore, it is impossible to separate the contribution of these transitions as $E_1 \rightarrow A$ and $E_1 \rightarrow E_1$ in the MCD.

The transition F2 = $E_1 \rightarrow (A + E_2)$ consists of two transitions: $E_1 \rightarrow A$ with the theoretical value $\Delta g_{CM} = -10$ and Gr1 ($J = 8$, $M_J = 4$, $g_{CM} = 10$, E_1) → ($J = 3$, $M_J = 5$, $g_{CM} = 5$, E_2) with a theoretical value of $\Delta g_{CM} = -5$ (Tables III and IV). The splitting sign coincides with that in the experiment, but the splitting value is much smaller (Table I). The accuracy of determining the amplitude of the weak line F2 (Fig. 2) is low, because it is against the background of the strong line f5. The F2 amplitude is necessary to calculate the

splitting. However, the deviation from theory is too large to attribute it to experimental error. Perhaps this is because, in addition to the Zeeman splitting of each of the transitions $E_1 \rightarrow A$ and $E_1 \rightarrow E_2$, there is also a splitting between these transitions, which contributes to the measured magnetic splitting.

5. CONCLUSION

The magnetic circular dichroism (MCD) and absorption spectra of multiferroic $HoFe_3(BO_3)_4$ in the region of f–f transitions $^5I_8 \rightarrow {}^5F_2$ and $^5F_3$ are measured at a temperature of 90 K. The absorption spectra are decomposed into Lorentzian components, and the transition intensities are obtained. The MCD and absorption spectra are used to determine the Zeeman splitting of transitions that are spectrally well-resolved. The MCD spectra and Zeeman splitting are theoretically analyzed in the free-atom wave function $|J, \pm M_J\rangle$ approximation by using the concept of a crystalline quantum number. It is found that the selection rules for the crystalline quantum number μ, which were in good agreement with the symmetry selection rules for ions with a half-integer moment, contradict them for ions with an integer moment. The selection rules for μ are modified, such that this contradiction is eliminated. Using the modified concept, the Zeeman splitting of some transitions were calculated, which were in satisfactory agreement with the experiment, that confirmed the validity of this concept. Anomalously intense vibronic satellites of electronic transitions from the excited ground multiplet sublevels are discovered, while the electronic transitions themselves are not observed. This corresponds to centrosymmetric local symmetry in the initial states and to vibronic parity-allowance of f–f transitions.

ACKNOWLEDGMENTS

The study was supported by the Russian Foundation for Basic Research, grant No. 19–02–00034, and also by the Krasnoyarsk Krai Russian Foundation for Basic Research and the Krasnoyarsk Krai Regional Fund of Science as part of project No. 19–42–240003 on "The influence of the local environment on the magneto-optical properties of f–f transitions in rare-earth aluminoborates and ferroborates."

REFERENCES

[1]R. P. Chaudhury, F. Yen, B. Lorenz, Y. Y. Sun, L. N. Bezmaternykh, V. L. Temerov, and C. W. Chu, Phys. Rev. B **80**, 104424 (2009).
[2]A. M. Kadomtseva, Y. F. Popov, G. P. Vorobiev, A. P. Pyatakov, S. S. Krotov, K. I. Kamilov, V. Y. Ivanov, A. A. Mukhin, A. K. Zvezdin, A. M. Kuzmenko, L. N. Bezmaternykh, I. A. Gudim, and V. L. Temerov, FNT **36**, 640 (2010) [Low Temp. Phys. **36**, 511 (2010)].
[3]D. A. Erofeev, E. P. Chukalina, L. N. Bezmaternykh, I. A. Gudim, and M. N. Popova, Opt. Spektrosc. **120**, 558 (2016).
[4]C. Ritter, A. Vorotynov, A. Pankrats, G. Petrakovskii, V. Temerov, I. Gudim, and R. Szymczak, J. Phys. Condens. Matter **20**, 365209 (2008).
[5]A. Pankrats, G. Petrakovskii, A. Kartashev, E. Eremin, and V. Temerov, J. Phys.: Condens. Matter **21**, 436001 (2009).
[6]A. V. Malakhovskii, S. L. Gnatchenko, I. S. Kachur, V. G. Piryatinskaya, and I. A. Gudim, Fiz. Nizk. Temp. **43**, 764 (2017) [Low Temp. Phys. **43**, 610 (2017)].
[7]A. V. Malakhovskii, S. L. Gnatchenko, I. S. Kachur, V. G. Piryatinskaya, and I. A. Gudim, Phys. Rev. B **96**, 224430 (2017).
[8]A. V. Malakhovskii, A. L. Sukhachev, A. Y. Strokova, and I. A. Gudim, Phys. Rev. B **88**, 075103 (2013).
[9]A. V. Malakhovskii, A. L. Sukhachev, V. V. Sokolov, T. V. Kutsak, V. S. Bondarev, and I. A. Gudim, J. Magn. Magn. Mater. **384**, 255 (2015).
[10]V. V. Sokolov, A. V. Malakhovskii, A. L. Sukhachev, and I. A. Gudim, Opt. Mater. **94**, 35 (2019).
[11]A. V. Malakhovskii, S. L. Gnatchenko, I. S. Kachur, V. G. Piryatinskaya, A. L. Sukhachev, and I. A. Gudim, J. Alloys Compd. **542**, 157 (2012).
[12]A. V. Malakhovskii, V. V. Sokolov, and I. A. Gudim, J. Alloys Compd. **698**, 364 (2017).
[13]A. V. Malakhovskii, V. V. Sokolov, and I. A. Gudim, J. Magn. Magn. Mater. **465**, 700 (2018).
[14]M. A. Elyashevich, *Spectra of Rare Earths* (GITTL, Moscow, 1953).
[15]A. V. Malakhovskii, S. L. Gnatchenko, I. S. Kachur, V. G. Piryatinskaya, and I. A. Gudim, J. Magn. Magn. Mater. **476**, 177 (2019).
[16]V. I. Zinenko, M. S. Pavlovskii, A. S. Krylov, I. A. Gudim, and E. V. Eremin, J. Exp. Theor. Phys. **117**, 1032 (2013) [ZhETF **144**, 1174 (2013)].

Translated by AIP Author Services